

Article

## Assessment of Groundwater Chemistry and Status in a Heavily Used Semi-Arid Region with Multivariate Statistical Analysis

Xuedi Zhang <sup>1,2,\*</sup>, Hui Qian <sup>1,2</sup>, Jie Chen <sup>1,2</sup> and Liang Qiao <sup>1,2</sup>

<sup>1</sup> School of Environmental Science and Engineering, Chang'an University, No. 126, Yanta Road, Xi'an 710054, Shaanxi, China; E-Mails: qianhui@chd.edu.cn (Q.H.); chenjie0705@gmail.com (C.J.); qiang\_liang@foxmail.com (Q.L.)

<sup>2</sup> Key Laboratory of Subsurface Hydrology and Ecology in Arid Areas, Ministry of Education, No. 126 Yanta Road, Xi'an 710054, Shaanxi, China

\* Author to whom correspondence should be addressed; E-Mail: zhangxuedi2007@163.com; Tel.: +86-29-82339327; Fax: +86-29-82339952.

Received: 16 April 2014; in revised form: 9 July 2014 / Accepted: 16 July 2014 /

Published: 25 July 2014

---

**Abstract:** This hydrogeological study assessed the quality of phreatic water supplies across the semi-arid, traditional agricultural region of the Yinchuan region in northwest China, near the upper reaches of the Yellow River. We analyzed the chemical characteristics of water collected from 39 sampling stations before the 2011 summer-autumn irrigation period, using multivariate statistical analysis and geostatistical methods. We determined which factors influence the composition of groundwater, using principal component analysis (PCA) and two modes of cluster analysis. PCA showed that the most important variables in the study area were the strong evaporation effect caused by the dry climate, dissolution of carbonate minerals and those containing  $F^-$  and  $K^-$ , and human activity including the treatment of domestic sewage and chemical fertilization. The Q-mode of cluster analysis identified three distinct water types that were distinguished by different chemical compositions, while the R-mode of analysis revealed two distinct clusters of sampling stations that appeared to be influenced by distinct sets of natural and/or anthropogenic factors.

**Keywords:** multivariate analysis; principal component analysis; cluster analysis; ground water; water quality; Yinchuan region; drought conditions

---

## 1. Introduction

Groundwater resources are a central source of drinking water around the world, because they are often good quality, difficult to pollute, widely distributed, and adjust throughout the year [1–4]. China is no exception, and relies greatly on these water resources. In the country's northwest, water for drinking, industrial uses, and irrigation comes mainly from groundwater, which thus plays an essential role in development [5]. With the rapid development of China's economy, the gap between water supply and demand in the northwest is widening each year. In many regions, growing water shortages and the pollution of shallow groundwater seriously restrict economic development [1,3,4], especially in the Yinchuan plain of Ningxia Province. Given the presence of few rivers at a low density, the region relies on artificial irrigation, via diversion of water from the Yellow River through a network of canals and ditches [5]. As contaminants and ions contained in soils dissolve into irrigation water, they infiltrate phreatic water, causing water quality to decline in some regions [3,5].

Groundwater hydrochemistry can be affected by multiple natural factors, such as chemical reactions between water and soil or sediments, biochemical reactions, and surface water–groundwater interactions, as well as human activities [1–3]. The industrial and municipal wastewater, whether treated or not, is a constant source of pollution that influences groundwater hydrochemistry. Additionally, groundwater may be affected by non-point sources of pollution, caused by surface and subsurface runoff from irrigation water and waste treatment plants in urban areas [3,4]. These human impacts on groundwater chemistry have been documented extensively [5–7]. Phenomena such as increasing industrialization, urbanization, agricultural irrigation, water pollution, and changes in irrigation practices (e.g., the channel line project and dredging of discharge ditches) greatly influence the phreatic water resources of Yinchuan region and may therefore alter water hydrochemistry.

Phreatic water is the main source for domestic and irrigation uses in the Yinchuan region, especially in villages. The over-populated area has traditionally depended on agriculture, with activities such as vegetable and greenhouse cultivation continuing year round [5]. Along with the aforementioned factors, the pumping of water from the Yellow River adds a further pressure to groundwater management. Water levels vary dramatically, influencing the amount that can be diverted from the River. Phreatic water in the region is characterized by a variable regime of recharging with annual irrigation. In these systems, artificial perturbations from irrigation (*i.e.*, fluctuations of the amount and quality of diverted water), population expansion, excess exploitation of groundwater, and other human activities have greatly changed and/or influenced the evolution of the water chemistry and hydrochemical characteristics of natural water in the Yinchuan region. Human intervention has resulted in complicated spatial-temporal changes in the quantity and quality of phreatic water, giving rise to a unique artificial ecosystem. These pressures make understanding the dynamics of phreatic water hydrochemistry in the region relatively more complex.

The goal of this study was to determine the factors influencing phreatic water quality in Yinchuan, and measure its current status, to facilitate sound water management in the region. We used multivariate statistical techniques as they have proven useful for summarizing water-quality data [4,8]. Our specific objectives were to: (1) assess the chemical characteristics of phreatic water in order to identify the factors that affect the region's phreatic water chemistry; (2) use principal component analysis (PCA) to identify the main drivers of phreatic water hydrochemistry; and (3) use cluster

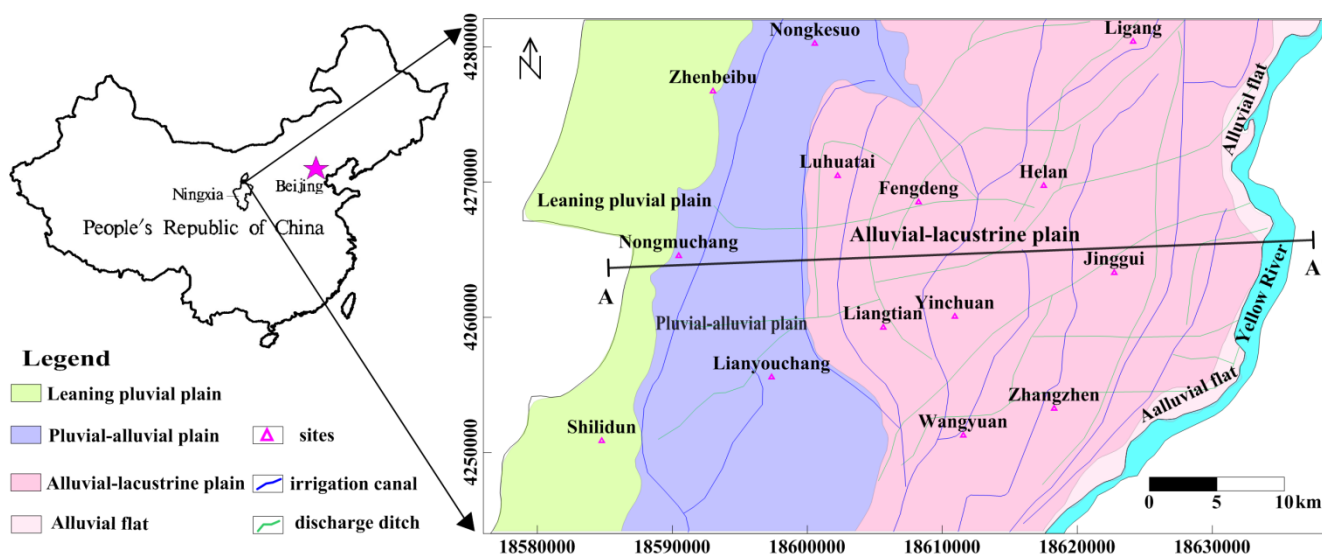
analysis (CA) to identify distinct water groups and assess different characteristics and the factors that influence them.

## 2. Study area

### 2.1. Location

The study area is located in the middle of the Yinchuan plain, in northwest China, near the upper reaches of the Yellow River. It is bounded by Helan Mountain in the west, and the Yellow River's western bank in the east. It measures 42–52 km wide from east to west and 38 km long from south to north, with a total area of 1836 km<sup>2</sup> (Figure 1).

**Figure 1.** Location of the study area and landforms in Yinchuan, Ningxia Province, China.



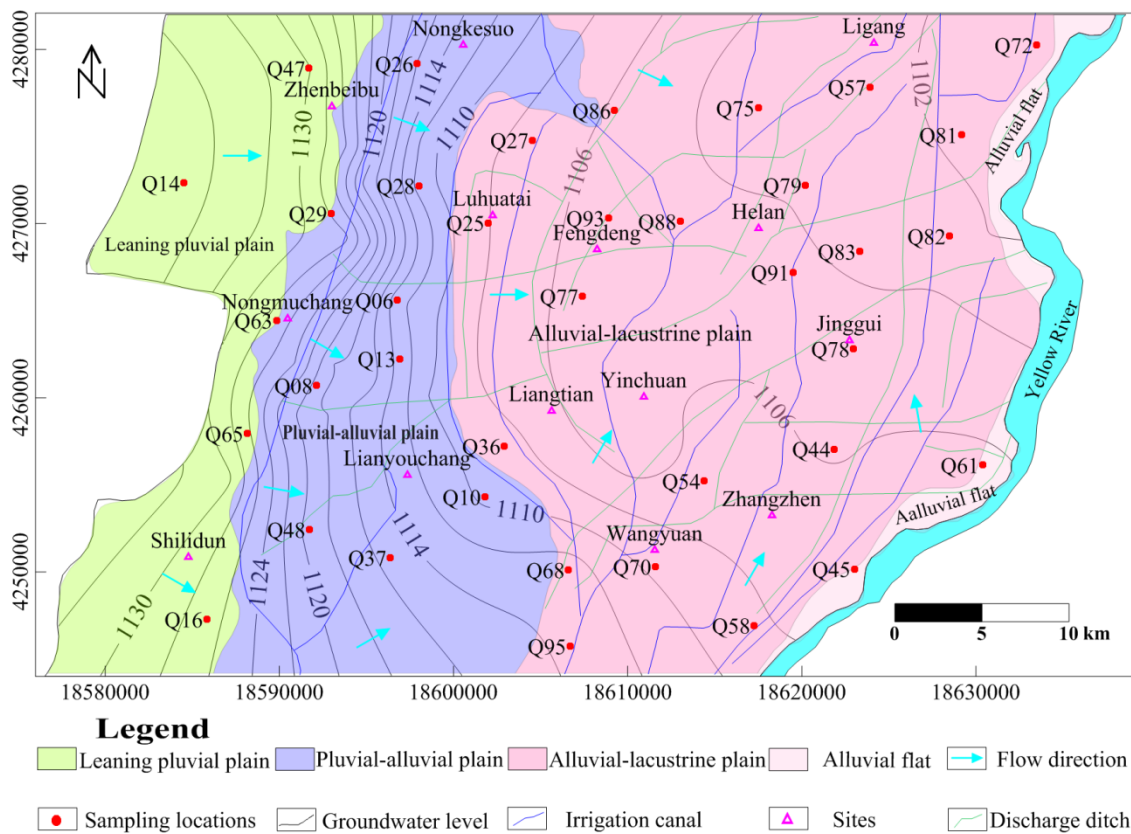
The Yinchuan region has an arid to semi-arid climate within the north temperature zone, with a long winter, short summer, less rain and more frequent droughts, ample sunshine, high wind and evaporation, and dramatic temperature changes. According to monitoring data from 1951 to 2010, annual precipitation is 191.9 mm, with 70% of it concentrated from July to September, and the average annual evaporation is 1582.8 mm, more than 8 times the amount of precipitation [9].

### 2.2. Hydrogeology

The elevation of the study area is higher in the west and lower in the east, ranging from approximately 1100 m to 1200 m above mean sea level, the lowest area in Ningxia. Landforms show a zonal distribution, sloping from a leaning pluvial plain at the foot of Helan Mountain in the west, to the pluvial-alluvial plain of the Yellow River, and alluvial-lacustrine plain and alluvial flat in the east (Figure 2). The Yinchuan Plain was formed by deposition of river, lake and flood sediments over a Cenozoic fault basin. It is a graben basin based on the evolution of the Helan tectonic belt and the Helan tectonic belt went through the tension and closing of the structure evolution many times from Mesoproterozoic Era to Cenozoic era, with rising and sink processes. First, the tensional fault is formed along the passive continental margin during Mesoproterozoic Era, with basic magmatic rising

activities along the fault, so the tensional fault filled with the littoral clastic rocks and carbonate rocks, basic volcano rocks depositing in some places. Then, this ancient fault expanded again and developed into a collision rift zone in the late Paleozoic, filling with paralic coal-bearing strata and terrestrial clastic rocks. The Helan mountain depression basin is expanded by the Alashan block, thrusting to the east after the Triassic period, filled with very thick deposition of lake, lake delta, alluvial fan. Lastly, the basin subsided greatly by compression in late Mesozoic and expanded to the west gradually. Yinchuan basin continued subsided and the west boundary has been extended to the east of Helan mountain during the late Tertiary period [10,11]. Therefore, the Yinchuan basin is complete and the maximum thickness of Quaternary sediments in the study area is 2000 m [12]. Data from drilling and diverse geological studies show that the pore water in sedimentary rocks of the Yinchuan region is divided into two zones: a single phreatic water zone and a multilayered structure area (Figure 3). The phreatic water zone is mainly in the west near Helan Mountain, with soils composed of gravel, sand and clay. The second zone includes all other areas, characterized by three aquifer layers within a depth of 250 m: moving down from the surface they are phreatic aquifer, upper confined aquifer and lower confined aquifer, with nearly continuous, 3–10 m-thick aquitards between them [9].

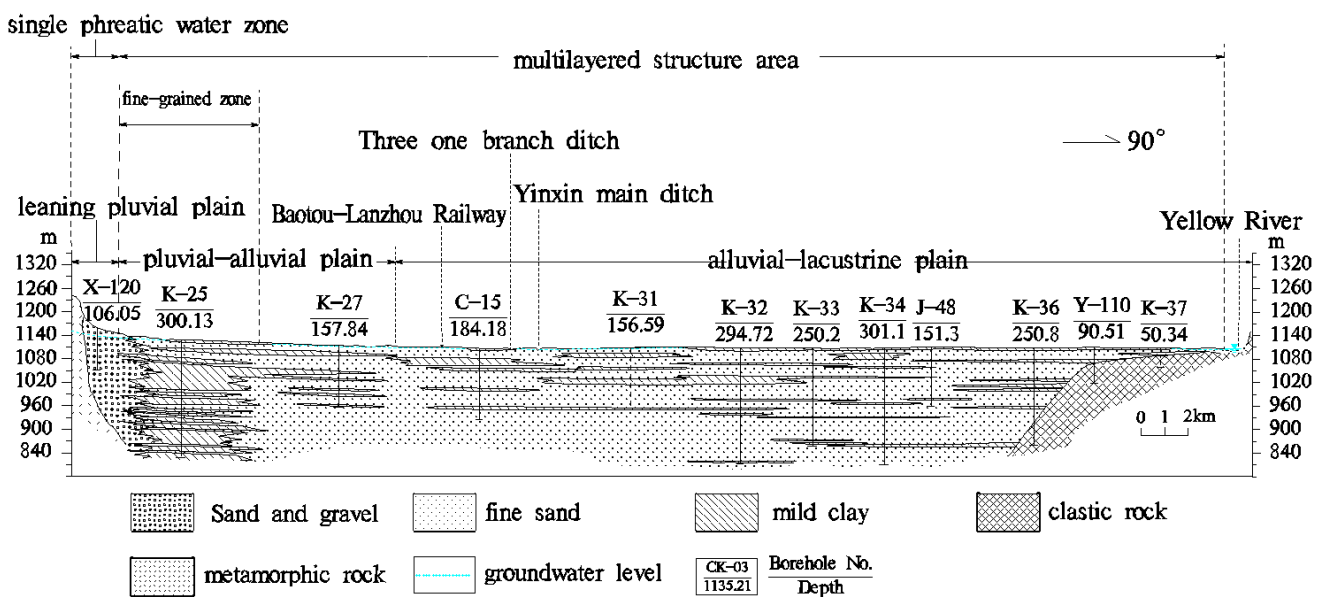
**Figure 2.** Hydrogeological map of phreatic aquifer and sampling stations in the study area (m).



Hydraulic head measurements indicate a successive variability in the hydrodynamic relationship among the geological units that constitute the groundwater level of phreatic aquifer, namely the leaning pluvial plain, pluvial-alluvial plain, alluvial-lacustrine plain and alluvial flat. As depicted in Figure 2, the groundwater runoff of phreatic aquifer flows from west to east in general, but the runoff directions and runoff conditions possess certain differences in different regions. In the leaning pluvial

plain, groundwater flows from west to east and the hydraulic gradient is larger, at 0.07%–0.15%. Along the flow path, because of the existence of fine-grained zone (Figure 3), located between leaning pluvial plain and the pluvial-alluvial plain, groundwater runoff is blocked and hydraulic gradient increases significantly, reached 3%–5%. The direction of groundwater runoff of phreatic aquifer in the alluvial-lacustrine plain diverts into from southwest to northeast and hydraulic gradient decreases significantly, down to 0.07%–0.05%, suggesting that phreatic water flows very slowly in this area (Figure 2). Similar to phreatic aquifer, groundwater runoff of confined water flows mainly from west to east and the hydraulic gradient is relatively large. In order to supply the consumption of industrial and drinking of Yinchuan city, the long-term, concentrated exploitation (212 wells) of groundwater from confined aquifer ( $8.7 \times 10^7 \text{ m}^3/\text{a}$ , accounting for 44.03% of the total pumping ( $1.98 \times 10^8 \text{ m}^3/\text{a}$ , which were groundwater source areas), has formed a depression cone in the confined aquifer in area between Liangtian and Luhutai, where groundwater flows down to the center of depression cone and phreatic water recharges confined water for a difference in hydraulic head. However, because hydraulic head of confined aquifer is higher than phreatic aquifer's, confined water will supply phreatic aquifer in other parts of the study area.

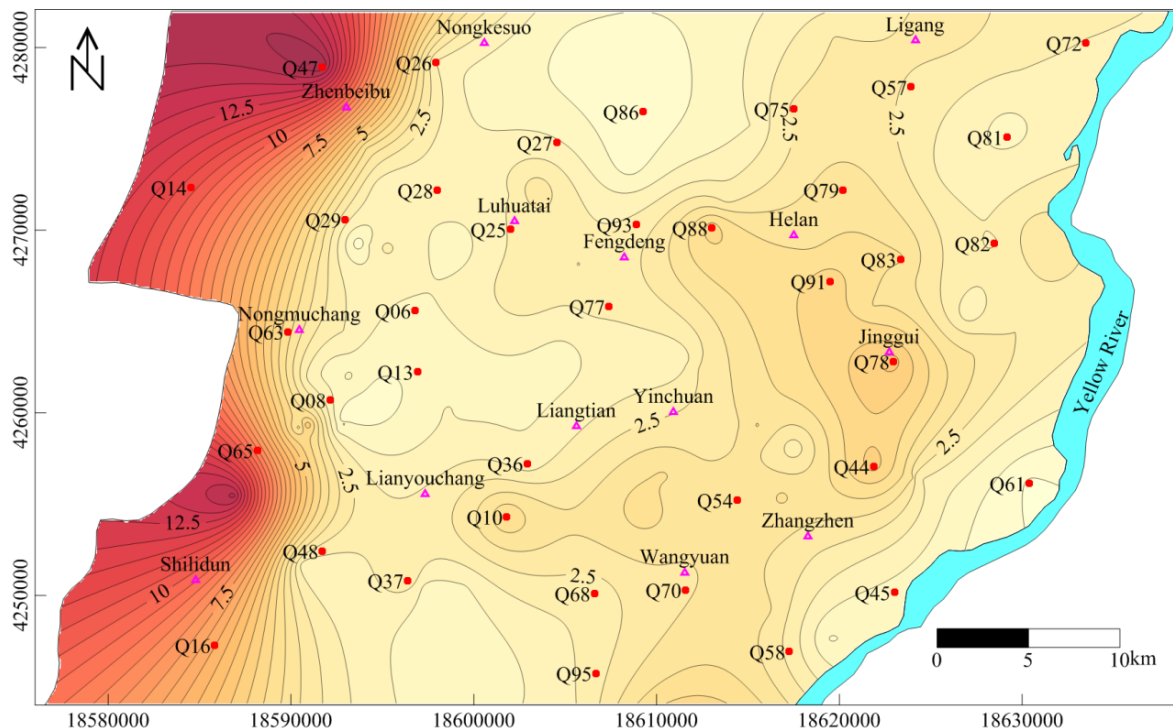
Figure 3. Hydrogeological cross section from A to A'.



Within the region's dense network of agricultural land, canals, and ditches are many scattered lakes, but few rivers. Recharge of phreatic water therefore occurs mainly via seepage from irrigation canals, accounting for more than 80% of the total recharge (about  $6.5 \times 10^8 \text{ m}^3/\text{a}$ ), and to a lesser extent from precipitation (about  $6.2 \times 10^7 \text{ m}^3/\text{a}$ ). Summer-autumn irrigation occurs annually from late April to late September, and winter irrigation is from late October to the middle of November (Figure 1). Field studies [9,12] have assessed the depth of phreatic water in the alluvial-lacustrine plain at 1–3 m in spring (before the summer-autumn irrigation), and mostly less than 2 m (Figure 4). Due to the groundwater's shallow depth, slow movement, and the lithology of the aeration zone, evaporation is intensive and accounts for more than 50% of the total discharge (about  $6.5 \times 10^8 \text{ m}^3/\text{a}$ ) of phreatic water (Figure 4). Another key pathway is via drainage ditches that leads ultimately to the

relatively stable, except when their water levels increase during flood periods. They include the Yinxin main ditch, the second drainage ditch and the Yong'er main ditch in the study area.

**Figure 4.** Distribution of groundwater depth (m) (March 2011).



Ecosystems of the Yinchuan region are affected seriously by numerous human activities, such as farming, irrigation, animal husbandry, fisheries, and the extraction of groundwater from aquifers. Water diversion for irrigation from the Yellow River to the Yinchuan Plain has occurred for more than 2000 years [13]. The average amount of water moved from the River to the plain over the last 20 years is  $57.46 \times 10^8 \text{ m}^3/\text{a}$ , 21.7 times the water availability from precipitation and inflow of groundwater [13]. Average salinity of the Yellow River water is 0.4 g/L. This long-term practice has increased the water table across the whole plain, and caused more intensive evaporation and hence a higher concentrations of ions in groundwater [9]. Wells on the alluvial-lacustrine plain, especially east of the Tanglai Canal, are less sensitive to rainfall infiltration, but irrigation and extraction are supported mainly by irrigation waters [5]. The main pollution sources of the study area are the point source pollution as industrial factories, non-point source pollution as the agricultural production for using chemical fertilizers and pesticide, and linear pollution sources as drainage ditches accepting industrial and municipal wastewater.  $\text{NH}_4^+$  pollution comes mainly from farm planting for using chemical fertilizers and pesticide, livestock breeding and the diverting water from Yellow River.

### 3. Materials and Methods

#### 3.1. Sampling Locations and Analytical Procedures

Samples of phreatic water were collected from 39 wells in 2011, before the summer-autumn irrigation period. They were labeled with a 3-character code, QAB, where Q is phreatic water and AB

is the two-digit number of the sampling station (Figure 2). Water temperature and pH were measured at each station. Water was collected in pre-cleaned 1 L plastic polyethylene bottles for physicochemical analysis, after a thorough rinse of the bottle with well water. Handling and preservation of samples followed the Standard Examination Methods for Drinking Water (Ministry of Health of the People's Republic of China, 2006) to maximize quality and consistency [14]. A duplicate sample from each station was acidified to pH 2 with the addition of HNO<sub>3</sub>, to assess the constituent cations. In the laboratory of Ningxia Monitoring Station for the Geological Environment, we analyzed sampled by measuring major ions (Na<sup>+</sup>, Ca<sup>2+</sup>, Mg<sup>2+</sup>, HCO<sub>3</sub><sup>-</sup>, SO<sub>4</sub><sup>2-</sup> and Cl<sup>-</sup>), total dissolved solids (TDS), total hardness (TH), K<sup>+</sup>, NH<sub>4</sub><sup>+</sup>, NO<sub>3</sub><sup>-</sup> and fluoride (F<sup>-</sup>), using standard procedures recommended by the Chinese Ministry of Water Resources, listed as appendix in Table A 1.

We checked those measurements for accuracy by calculating percent charge balance errors (%CBE), with Equation (1).

$$\%CBE = \frac{\sum cations - \sum anions}{\sum cations + \sum anions} \times 100\% \quad (1)$$

where all cations and anions are expressed as milliequivalents per liter. We verified that the TDS measure did not differ much from the sum of all seven major ions. All samples had a small relative error (%CBE) of < ±5%, therefore all 39 samples were used in analyses.

### 3.2. Multivariate Statistical Analysis

Multivariate statistical techniques, such as PCA and CA, are often used as “unbiased methods” to summarize associations between samples and/or variables [15,16]. Such associations based on similar magnitudes and variations in chemical and physical composition may reveal the effects of climate or human activity on water quality. Hierarchical agglomerative CA groups samples by linking their similarities, and thus can be used to illustrate the overall similarity of variables within a dataset. In order to avoid misclassification due to wide differences in the dimensions of data, we standardized measurements with z-scale transformation [17,18]. Standardization tends to increase the influence of factors with small variance, and vice versa. All mathematical and statistical computations were made using the Statistical Package for Social Sciences software (SPSS 16.0) [19].

PCA was used to detect associations among variables (standardized data), thus reducing the number of dimensions in the data table. This was accomplished by diagonalization of the correlation matrix, which transformed the 13 original variables into 13 uncorrelated (orthogonal) ones, *i.e.*, weighted linear combinations of the original variables, or Principal Components (PCs). The eigenvalues of the PCs are a measure of their associated variance, the most participation of the original variables in the PCs is shown by the loadings, and the individual transformed observations are called scores. To reduce the overlap between original variables in each PC, a varimax rotation was conducted [17]. The dataset for PCA included all 13 measures, thereby providing a simultaneous analysis of the whole hydrochemical dataset.

CA is an unsupervised pattern recognition technique that reveals the intrinsic structure or underlying behavior of a dataset, without making a priori assumptions about the data, in order to classify objects into groups or clusters, based on their similarity. There are two types of CA: R-mode

and Q-mode [20]. Q-mode CA can be used to assess common water quality data, grouping samples into clusters of distinct quality, based on similarities (*i.e.*, Euclidean distance) in their hydrochemistry. R-mode CA is often used to assess the associations among different variables. In hydrological studies, it has been used to determine the association among water quality parameters, and ultimately the sources and processes that influence them [21–24]. We chose Ward’s method of hierarchical agglomerative CA, a powerful grouping mechanism that uses squared Euclidean distances as a measure of similarity between samples and/or variables (standardized data), has a small space distorting effect, and uses more information about cluster contents than other hierarchical methods [18].

## 4. Results and Discussion

### 4.1. Hydrochemical Characteristics

Analysis of the 13 hydrochemical variables of phreatic water in the study area is summarized in Table 1. The water samples were weakly alkaline, with a pH range of 7.71–8.38. Concentrations of the principal ions varied greatly, with coefficients of variation varying from 0.4 to 1.9, especially  $\text{Na}^+$ ,  $\text{Mg}^{2+}$ ,  $\text{SO}_4^{2-}$  and  $\text{Cl}^-$ . For example, the concentration of TDS varied from 272 to 5664 mg/L (mean 1065 mg/L). Measures of all major ions exceeded China’s acceptable limits for groundwater quality (Bureau of Quality and Technical Supervision of China 1994). Most samples from the central and eastern parts of the study area had high TDS values above 1000 mg/L, along the Yellow River (Figure 5a), indicating they are unsuitable for drinking. TH measured as  $\text{CaCO}_3$  varied from 146 to 2845 mg/L, (mean 509 mg/L), and exceeded 450 mg/L in most areas (except the west and small parts of the central study area), suggesting very hard water that is unsuitable for drinking (Figure 5b). Generally, the groundwater from the samples at higher elevation contained mostly  $\text{Ca}^{2+}$  and  $\text{HCO}_3^-$ , and the concentrations of  $\text{Na}^+$ ,  $\text{SO}_4^{2-}$  and  $\text{Cl}^-$  increased at lower elevations due to mineral dissolution along the paths of groundwater flow [5].

**Table 1.** Descriptive statistics of hydrochemistry in Yinchuan, China.

Parameters	Phreatic water					Yellow river	National standard
	Category	Minimum	Maximum	Mean	SD	CV	/
pH	7.71	8.38	8.08	0.11	0.01	8.10	6.5–8.5
TH	146	2845	509	417	0.8	245	450
TDS	272	5664	1065	885	0.8	386	1000
$\text{Ca}^{2+}$	23.0	439.7	83.9	66.3	0.8	53.8	–
$\text{Mg}^{2+}$	23.3	509	85.7	81.4	0.9	27.9	–
$\text{K}^+$	1.5	17.0	4.9	3.4	0.7	3.0	–
$\text{Na}^+$	24.0	860	181	167	0.9	43.0	200
$\text{Cl}^-$	27.6	2592	222	406	1.8	55.2	250
$\text{SO}_4^{2-}$	35.2	986	214	184	0.9	83.6	250
$\text{HCO}_3^-$	220	1106	501	210	0.4	207	–
$\text{NO}_3^-$	0.0	21	2.1	4.4	2.0	–	20
$\text{NH}_4^+$	0.0	1.0	0.1	0.2	4.1	–	0.20
$\text{F}^-$	0.1	1.2	0.3	0.2	0.9	–	1

Note: Units: mg/L (except for pH).

**Figure 5.** Contour maps of hydrochemical measurements (mg/L) for phreatic water (a) TDS; (b) TH; (c)  $Mg^{2+}$ ; (d)  $Ca^{2+}$ ; (e)  $Na^+$ ; (f)  $Cl^-$ ; (g)  $SO_4^{2-}$ ; (h)  $HCO_3^-$ ; (i)  $NO_3^-$ ; (j)  $NH_4^+$ ; (k)  $F^-$ ; (l)  $K^+$ .

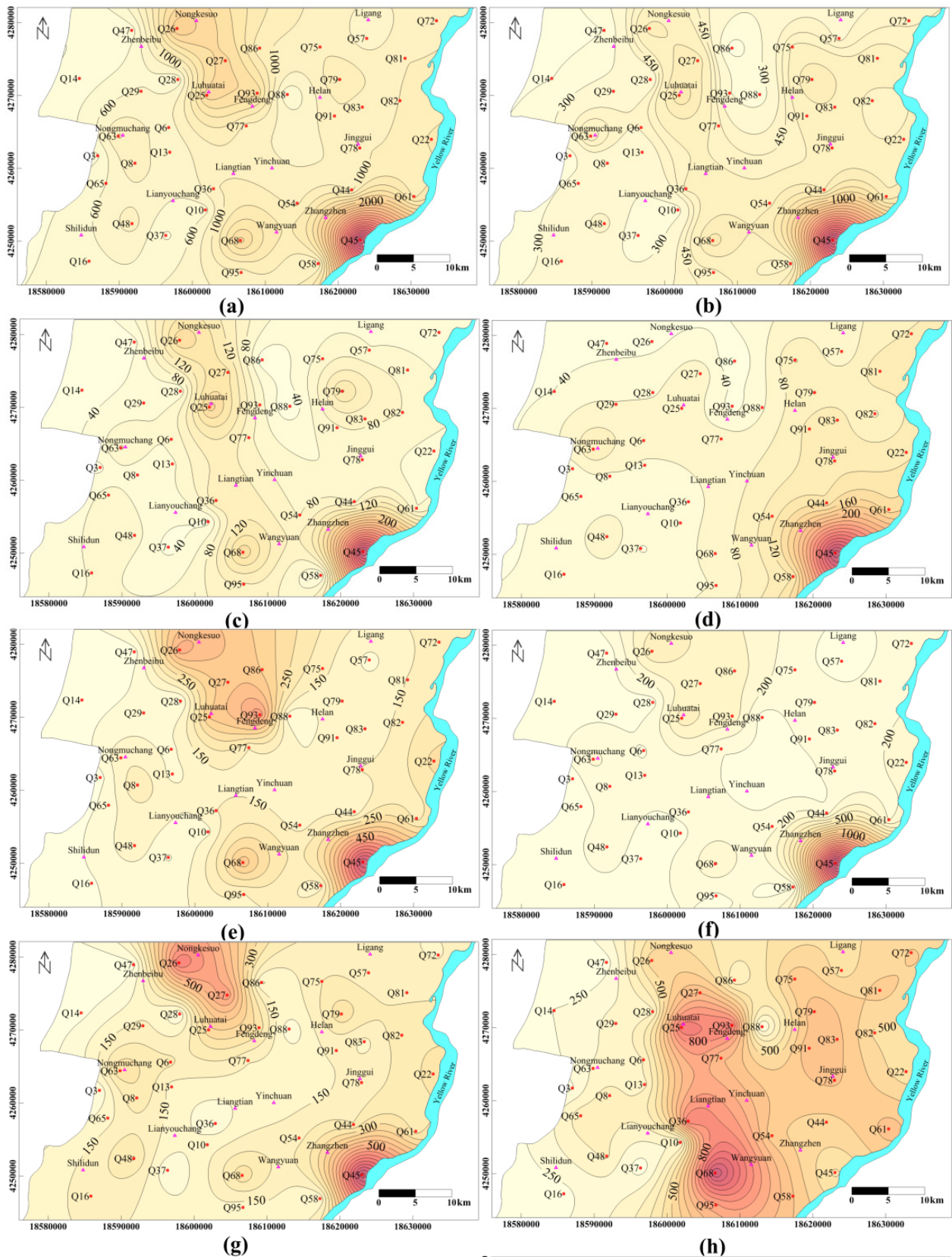
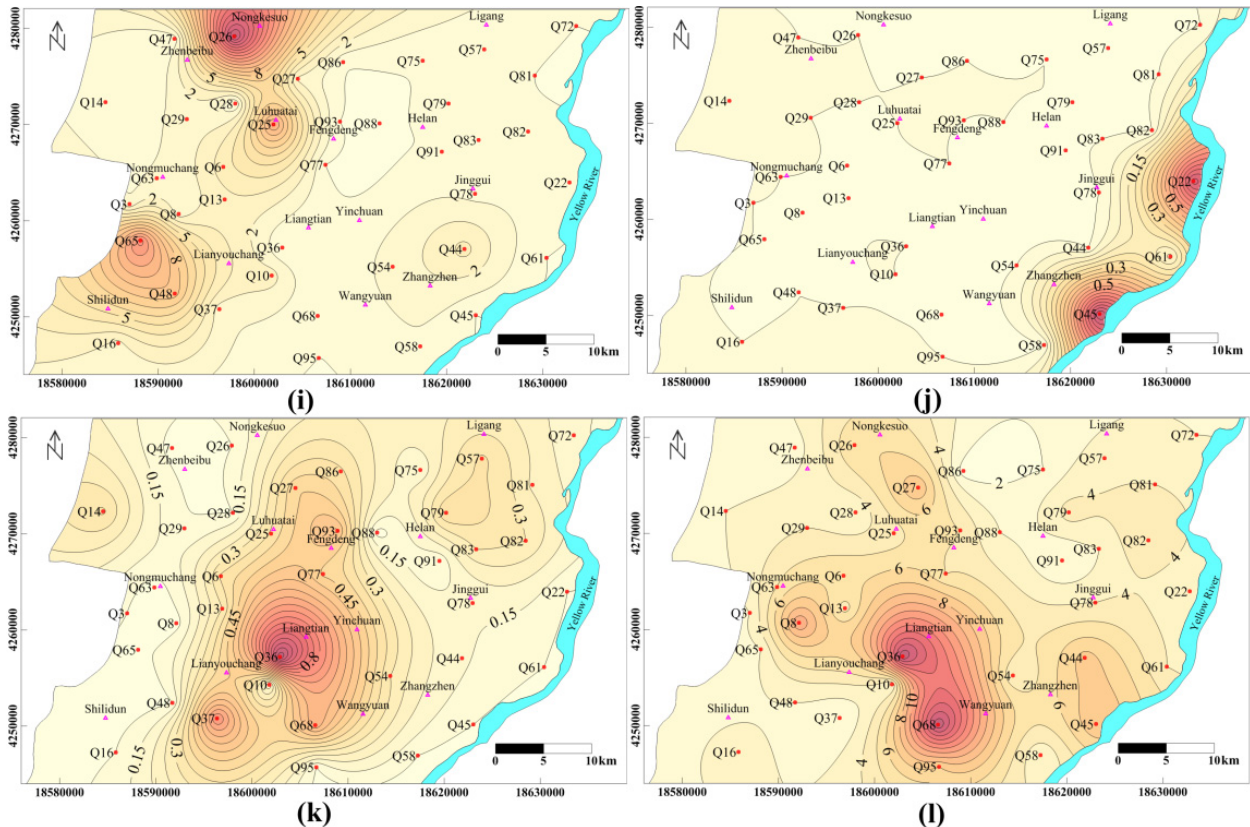


Figure 5. Cont.



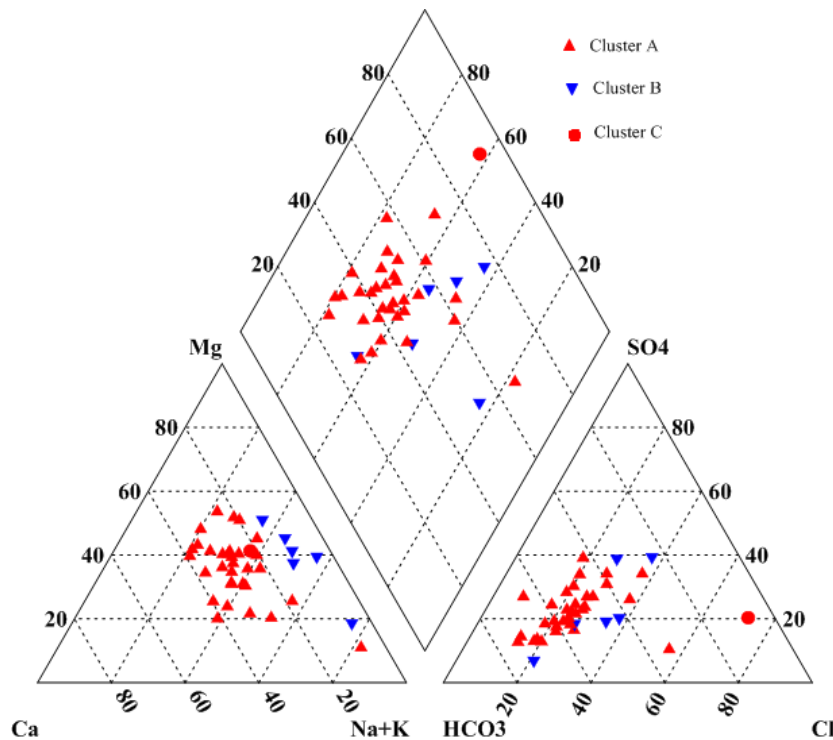
The spatial distribution of TH and  $Mg^{2+}$  were similar (Figure 5b,c), with higher values in the central and eastern areas. The spatial distribution of  $Ca^{2+}$  increased from the southwest and northwest parts of the study area to the east (Figure 5d).  $Na^+$ ,  $SO_4^{2-}$  and  $Cl^-$  concentrations were higher (beyond the acceptable limits) in the vicinity of Luhatai and Nongkesuo in the north, and Zhangzhen in the southeast, and lower in other parts of the study area (Figure 5e,f,g). Unusually high concentrations were found at three sample points: Q26, Q27 and Q45. The distribution of  $SO_4^{2-}$  increased from the outer parts of the study area toward the center (Figure 5g). Concentrations of  $HCO_3^-$  increased gradually from west to east, forming four areas of high concentration near sites Q25, Q36, Q68 and Q93 in the central (Figure 5h).  $NO_3^-$  concentrations were relatively high in the vicinity of Shilidun and Luhatai, beyond China's acceptable limits in Nongkesuo (in the north), and lower in other parts of the study area (Figure 5i). In contrast,  $NH_4^+$  concentrations were markedly higher in the banded areas along the Yellow River beyond the national limits for drinking water (Figure 5j).  $F^-$  concentrations had a very different distribution, being highest in the center and northeast (Figure 5k). Concentrations of  $K^+$  increased from the southwest and northwest toward the center, peaking in the northeast (Figure 5l).

Concentrations of nearly all major ions were highest near Q26, Q27 (in the north) and Q45 (in the southeast), which may have been caused by similar hydrogeochemical processes. Evaporation in this area is intense, and the groundwater depth is shallow at less than 2 m, while the extinction evaporation depth is 3 m; the amount of annual evaporation is 8 times that of precipitation [5,9,12]. Furthermore, the decrease in ion concentrations at lower elevations may be attributed to leakage from canals and the seepage of irrigation water, which have very low concentrations of dissolved ions. Local activities

such as sewage disposal and agricultural irrigation may further recharge the phreatic water levels, causing the quantity to change.

Piper trilinear diagrams are used commonly to identify hydrochemical patterns in ion data [5,19,25]. In terms of cations, most samples were plotted in the central zone of the right delta-shaped region of our Piper diagram (Figure 6), suggesting that some stations had sodium-type water while most were mixed-type. For anions, most samples were located in the left zone of the lower right delta-shaped region, indicating the dominance of bicarbonate-type water, while some stations had mixed-type.

**Figure 6.** Piper diagram of phreatic water drawn with AquaChem 4.0.



#### 4.2. Correlation among Parameters

The correlations among water-quality variables (Table 2) allow us to distinguish several relevant hydrochemical relationships. Measures of the major ions and trace elements, except for  $K^+$ ,  $HCO_3^-$ ,  $NO_3^-$  and  $F^-$ , were significantly and positively correlated with TDS. Concentrations of  $Cl^-$ ,  $SO_4^{2-}$ ,  $Na^+$  and  $Mg^{2+}$  were related, with correlation coefficients ( $r$ ) ranging from 0.805 to 0.919, implying that there is possibly a common cause for an increase in these ions. Concentrations of  $Ca^{2+}$  and  $Mg^{2+}$  were strongly correlated with TH ( $r = 0.928$  and  $0.953$ , respectively), which is intuitive as hardness is an approximate measure of  $Ca^{2+}$  and  $Mg^{2+}$ . TH was also strongly correlated with  $SO_4^{2-}$ , ( $r = 0.809$ ), and weakly correlated with  $HCO_3^-$  ( $r = 0.245$ ), implying that TH is essentially a permanent hardness. As calcite and dolomite dissolve and precipitate, concentrations of  $Ca^{2+}$  and  $Mg^{2+}$  increase, and  $HCO_3^-$  decreases, resulting in higher TH and lower TDS [26]. The correlation of  $Ca^{2+}$  with  $SO_4^{2-}$  was not as strong as that of  $Na^+$  and  $Mg^{2+}$ , so the dissolution of gypsum cannot be assumed as a main source of  $Ca^{2+}$  and  $SO_4^{2-}$ . Additional reactions involving  $Ca^{2+}$ , such as carbonate dissolution/precipitation and cation exchange, could account for the correlation with  $SO_4^{2-}$ .

**Table 2.** Correlation matrix of the 13 physico-chemical water parameters. The values are the correlations coefficients (*r*).

Catalog	pH	TH	TDS	Ca <sup>2+</sup>	Mg <sup>2+</sup>	K <sup>+</sup>	Na <sup>+</sup>	Cl <sup>-</sup>	SO <sub>4</sub> <sup>2+</sup>	HCO <sub>3</sub> <sup>-</sup>	NO <sub>3</sub> <sup>-</sup>	NH <sub>4</sub> <sup>+</sup>	F <sup>-</sup>
pH	1												
TH	<b>-0.50</b>	1											
TDS	<b>-0.57</b>	<b>0.935</b>	1										
Ca <sup>2+</sup>	<b>-0.41</b>	<b>0.928</b>	<b>0.792</b>	1									
Mg <sup>2+</sup>	<b>-0.51</b>	<b>0.953</b>	<b>0.952</b>	<b>0.771</b>	1								
K <sup>+</sup>	0.04	0.293	0.345	0.106	<b>0.415</b>	1							
Na <sup>+</sup>	<b>-0.54</b>	<b>0.742</b>	<b>0.929</b>	<b>0.568</b>	<b>0.805</b>	0.343	1						
Cl <sup>-</sup>	<b>-0.62</b>	<b>0.941</b>	<b>0.955</b>	<b>0.846</b>	<b>0.919</b>	0.216	<b>0.839</b>	1					
SO <sub>4</sub> <sup>2-</sup>	<b>-0.58</b>	<b>0.809</b>	<b>0.907</b>	<b>0.641</b>	<b>0.861</b>	0.277	<b>0.851</b>	<b>0.817</b>	1				
HCO <sub>3</sub> <sup>-</sup>	0.17	0.245	0.347	0.106	0.332	<b>0.557</b>	<b>0.438</b>	0.109	0.227	1			
NO <sub>3</sub> <sup>-</sup>	-0.27	0.00	0.126	-0.19	0.163	-0.033	0.173	0.044	0.344	-0.02	1		
NH <sub>4</sub> <sup>+</sup>	<b>-0.41</b>	<b>0.688</b>	<b>0.657</b>	<b>0.719</b>	<b>0.591</b>	0.046	<b>0.556</b>	<b>0.73</b>	<b>0.55</b>	-0.054	-0.11	1	
F <sup>-</sup>	0.243	-0.06	0.013	-0.22	0.071	<b>0.551</b>	0.092	-0.06	-0.11	<b>0.443</b>	-0.16	-0.17	1

Notes: **Correlation** = significant at the 0.01 level (2-tailed); *Correlation* = significant at the 0.05 level (2-tailed).

Notably, the chemical reactions within a groundwater system are numerous and highly complex. Although correlation analysis is a useful tool, it can provide only a general insight into phreatic water hydrochemistry [19]. To know more about the exact reactions taking place, more comprehensive analyses of aquifer mineralogy and groundwater flow are needed.

#### 4.3. Principal Component Analysis (PCA)

A Bartlett's sphericity test confirmed that the 13 variables were not orthogonal but rather were correlated (Bartlett  $\chi^2 = 1354$ , 78 df,  $p \leq 0.001$ ). This enables explanation of the variation in these hydrochemical data with a lower number of variables. Additionally, the Kaiser–Meyer–Olkin method (KMO) showed that the measure of sampling adequacy (MSA) was 0.623, indicating that the degree of correlation among the variables and the appropriateness of factor analysis was middling.

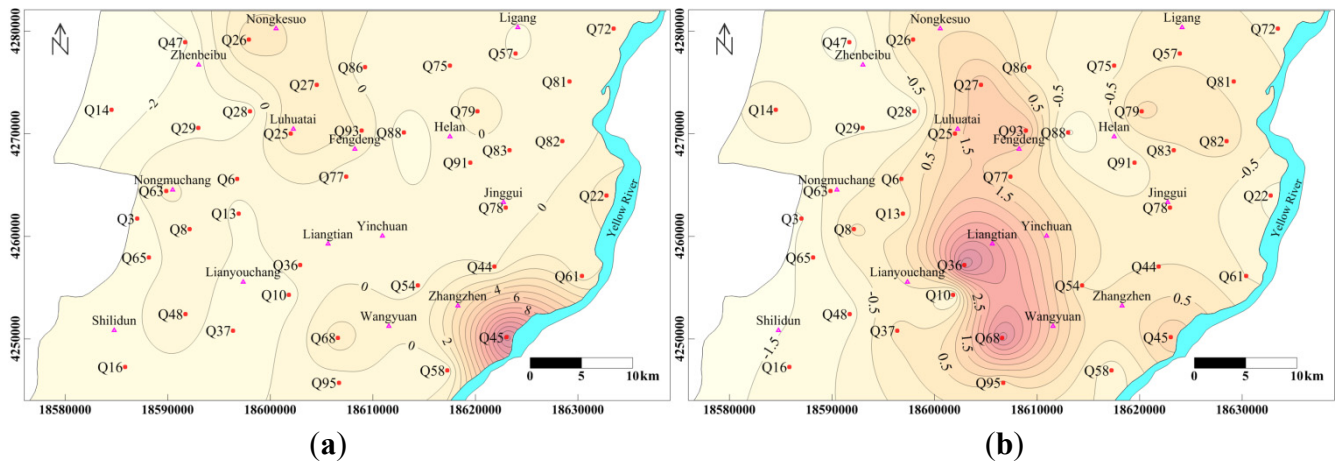
PCA considered the hydrochemical variables common to all 39 samples, including pH, TH, TDS, K<sup>+</sup>, Na<sup>+</sup>, Ca<sup>2+</sup>, Mg<sup>2+</sup>, HCO<sub>3</sub><sup>-</sup>, SO<sub>4</sub><sup>2-</sup>, Cl<sup>-</sup>, NH<sub>4</sub><sup>+</sup>, NO<sub>3</sub><sup>-</sup> and F<sup>-</sup>. The correlation matrix of the 13 variables (standardized data) revealed several relevant hydrochemical relationships that can help to interpret the primary factors that have influenced current water chemistry in the region [27]. Most variables were strongly correlated with more than one other component (Table 2). In PCA, the correlations among the variables were used to estimate PCs with common associations and associated constituent loadings on PCs [28]. To reduce the overlap between original variables in each PC, a varimax rotation was conducted [17]. The total variance explained by each PC, their loadings, and eigenvalues are shown in Table 3. Based on eigenvalues greater than 1, 4 PCs were extracted that accounted for 87.6% of the total variance in the original dataset (Table 3). The first two PCs explained for most of the variance, at 53.7% and 14.6%, respectively. While PCs 3 and 4 explained 11.2% and 8.1%.

**Table 3.** Loadings of variables on 4 Principal Components (PCs) of water quality measurements.

Variable	PC1	PC2	PC3	PC4
TH	<b>0.97</b>	0.04	−0.04	0.07
Cl <sup>−</sup>	<b>0.97</b>	0.06	0.03	−0.13
TDS	<b>0.97</b>	0.16	0.15	0.07
Mg <sup>2+</sup>	<b>0.93</b>	0.21	0.16	0.08
Ca <sup>2+</sup>	<b>0.90</b>	−0.18	−0.28	0.06
SO <sub>4</sub> <sup>2−</sup>	<b>0.86</b>	0.05	0.39	0.04
Na <sup>+</sup>	<b>0.84</b>	0.25	0.27	0.09
NH <sub>4</sub> <sup>+</sup>	<b>0.77</b>	−0.13	−0.25	−0.20
pH	<b>−0.59</b>	0.04	−0.37	0.57
F <sup>−</sup>	−0.12	<b>0.92</b>	−0.13	0.04
K <sup>+</sup>	0.24	<b>0.79</b>	0.03	0.26
NO <sub>3</sub> <sup>−</sup>	0.02	−0.10	<b>0.94</b>	−0.02
HCO <sub>3</sub> <sup>−</sup>	0.21	0.49	0.09	<b>0.76</b>
Eigenvalue	6.99	1.89	1.45	1.06
% of Variance explained	53.7	14.6	11.2	8.1
% Cumulative variance	53.7	68.3	79.5	87.6

PC1 was highly related to TH, Cl<sup>−</sup>, TDS, Mg<sup>2+</sup>, Ca<sup>2+</sup>, SO<sub>4</sub><sup>2−</sup> and Na<sup>+</sup>, indicating that these variables have common patterns. PC1 also had a strongly positive loading for NH<sub>4</sub><sup>+</sup>, implying an effect of human activity (e.g., domestic sewage, chemical fertilizers, such as NH<sub>4</sub>HCO<sub>3</sub>, CO(NH<sub>2</sub>)<sub>2</sub>, NH<sub>4</sub>NO<sub>3</sub>, (NH<sub>4</sub>)<sub>2</sub>SO<sub>4</sub>, Ca(H<sub>2</sub>PO<sub>4</sub>)<sub>2</sub> and KCl) on phreatic water. Further, it had a moderately negative loading for pH, showing that samples with high TDS and much more SO<sub>4</sub><sup>2−</sup>, so pH will drop. This can be interpreted as a strong evaporation effect due to the drought climate in this area. Major ions, such as Na<sup>+</sup>, Mg<sup>2+</sup>, Ca<sup>2+</sup>, SO<sub>4</sub><sup>2−</sup> and Cl<sup>−</sup>, are important components of TDS and/or TH.

Due to the fact that the majority of discharge from the phreatic aquifer occurs by evaporation, large amounts of salts remain in the soil and accumulate in phreatic water, lowering its quality. Compounds whose solubility products are small (e.g., the solubility product  $K_{sp}$  of CaCO<sub>3</sub> is  $4.96 \times 10^{-9}$  at 25 °C) can reach saturation and then precipitate [26], so the main ions that remain dissolved in phreatic water are Mg<sup>2+</sup>, Ca<sup>2+</sup>, Na<sup>+</sup>, SO<sub>4</sub><sup>2−</sup>, and Cl<sup>−</sup>. The loading of those ions on PC1 ranged from 0.84–0.97. As the concentration of K<sup>+</sup>, Na<sup>+</sup>, Ca<sup>2+</sup>, Mg<sup>2+</sup>, HCO<sub>3</sub><sup>−</sup>, SO<sub>4</sub><sup>2−</sup> and Cl<sup>−</sup> in the phreatic water gradually increases with TDS, groundwater will be under saturated with calcite, dolomite and gypsum, with respect to the solubility product. Therefore, we infer that PC1 reflected the strong evaporation effect, shallow groundwater sources, patterns of land use, and intensity of human activities in the Yinchuan region. Indeed, three parts of the region had high values of PC1: Luhuatai and Nongkesuo (in the north), and east of Zhangzheng along the Yellow River (Figure 7a), in which groundwater starts at shallow depth (Figure 4). In contrast, PC1 values were lower in the west, where larger groundwater depths are associated with less evaporation, so the water quality of phreatic water there is hardly affected by the external environment and human activities. The concentrations of ions there were also relatively lower and water type was relatively simpler, for example HCO<sub>3</sub>-Mg, HCO<sub>3</sub>-Mg.Ca and HCO<sub>3</sub>-Mg.Na types.

**Figure 7.** Spatial distribution of sampling stations by (a) PC1 scores and (b) PC2 scores.

Loadings on PC2 showed that  $F^-$  and  $K^-$  were most important for that component; in addition, the weak positive correlation of PC2 with  $HCO_3^-$  represents dissolution of minerals that contain  $F^-$  and  $K^-$ . Sampling stations in the center of the study area and southeast of Zhangzhen had high PC2 scores, which were otherwise relatively small. This suggests that there is strong dissolution of minerals with  $F^-$  and  $K^-$  in the central area (Figure 7b). The spatial pattern of PC2 scores was different from that of PC1, *i.e.*, the distribution of high PC2 scores was concentrated in the part of the study area with excessive exploitation of confined water (around Yinchuan City), where groundwater levels fluctuate greatly and the dissolution of mineral is common.

PC3 was greatly influenced by  $NO_3^-$ , related to the use of nitrate fertilizers used in irrigation. For example, nitrate measured at sampling station Q26 (near Nongkesuo, in the north) was 21.47 mg/L, the highest  $NO_3^-$  concentration that we found, significantly beyond Grade 3 of the water quality standards (Table 1; Figure 5j). The highest positive loading on PC4 was by  $HCO_3^-$ , indicating an influence of the dissolution of carbonate minerals.

#### 4.4. Cluster Analysis

##### 4.4.1. Q-Mode Cluster Analysis

The classified results of Q-mode CA are presented as dendrograms. For our results, an imaginary horizontal line (phenon line) is drawn across the dendrogram at a linkage distance of about seven reveals three distinct groups, clusters A through C (Figure 8), whose member sampling stations are listed in Table 4. Stiff diagrams for each cluster of water samples show the mean concentrations of their main constituent ions (Figure 8), which combined with the dendrogram and the summary of geochemical and physical data (Table 5) demonstrate that the three clusters are geochemically independent groups.

Each cluster appeared to have a distinct water quality, different from the other two groups. Looking at TDS for example, cluster A includes six subgroups, A1 to A6, where the average TDS concentration is 790 mg/L, and ranged from 272 to 1236 mg/L (characteristic of fresh water). Cluster B includes three subgroups, B1 to B3, with an average TDS of 1765 mg/L (ranging from 985 to 2200 mg/L), which is characteristic of moderately salty water influenced by evaporation and pollution. However,

Cluster C includes only one sample, Q45, with TDS of 5664 mg/L, characteristic of salt water. TDS, TH and most major ions (other than  $\text{Ca}^{2+}$  and  $\text{HCO}_3^-$ ) increased significantly from Cluster A to Cluster C, yet minor ions ( $\text{K}^+$ ,  $\text{NO}_3^-$  and  $\text{F}^-$ ) were most concentrated in Cluster B. There was no clear trend for  $\text{Ca}^{2+}$ , probably due to its involvement in so many complex reactions, including carbonate dissolution/precipitation and cation exchange. Similarly, by considering each of the other water quality variables (major ions, minor ions and trace elements), the water quality or chemistry associated with each cluster can be assessed in detail [27].

**Figure 8.** Dendrogram from cluster analysis (Q-mode) of water samples showing the division into three clusters and the stiff diagram of mean concentrations for each cluster.

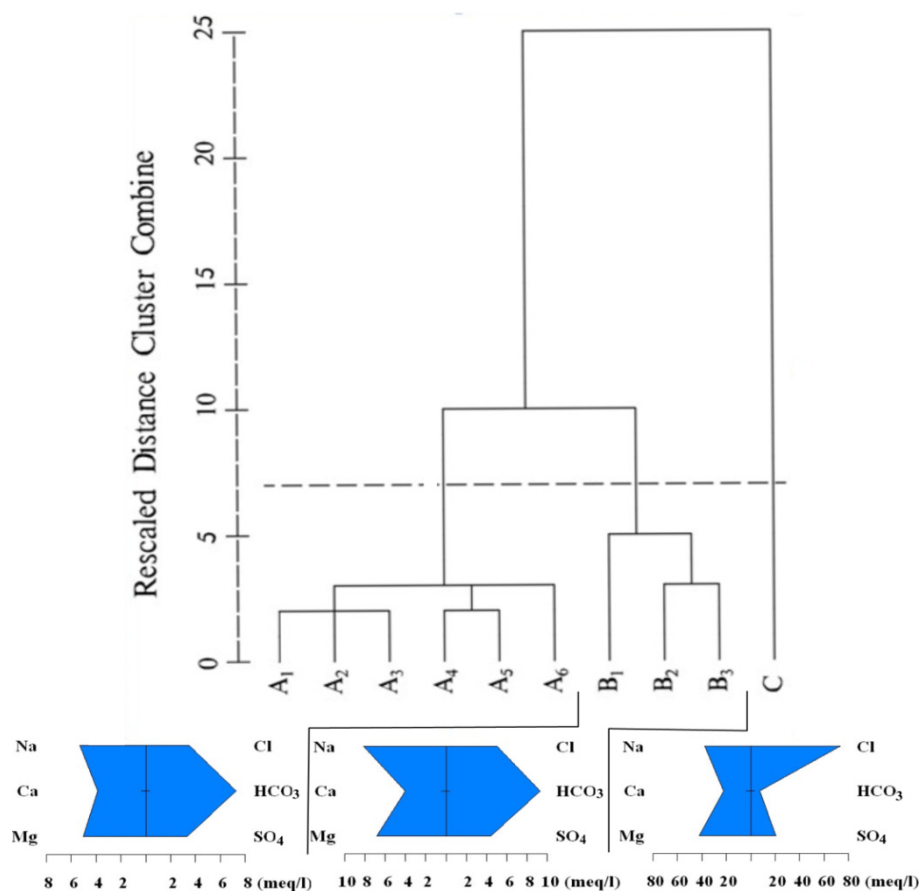


**Table 4.** Samples contained in each of the clusters of the dendrogram shown in Figure 8.

Cluster	Samples
A1	Q3,Q8,Q10,Q16, Q28,Q29, Q47,Q63,Q88
A2	Q48, Q65
A3	Q6, Q13, Q37, Q57, Q77, Q86
A4	Q14, Q82
A5	Q44,Q54, Q58,Q61,Q72,Q75,Q78,Q79,Q81,Q83,Q91,Q95
A6	Q22
B1	Q36, Q68,
B2	Q25, Q27, Q93
B3	Q26
C	Q45

**Table 5.** Mean concentrations of chemical parameters for different clusters of water samples.

Index	Cluster A	Cluster B	Cluster C
pH	8.10	8.06	7.71
TH	417	610	2845
TDS	790	1765	5664
Ca <sup>2+</sup>	78.0	56.0	439.7
Mg <sup>2+</sup>	60.9	147.4	508.7
K <sup>+</sup>	3.9	9.6	8.0
Na <sup>+</sup>	122	381	860
Cl <sup>-</sup>	123	351	2592
SO <sub>4</sub> <sup>2+</sup>	159	378	986
HCO <sub>3</sub> <sup>-</sup>	444	815	440
NO <sub>3</sub> <sup>-</sup>	1.53	5.76	0
NH <sub>4</sub> <sup>+</sup>	0.03	0.00	1.01
F <sup>-</sup>	0.21	0.55	0.10

Note: Units: mg/L (except for pH).

The water samples of Cluster A were dominated by magnesium, sodium and bicarbonate, however, calcium, chloride and sulfate were also present, and in high concentration in some areas. Therefore, the dominant hydrochemical facies are HCO<sub>3</sub>-Mg, HCO<sub>3</sub>-Mg.Na and HCO<sub>3</sub>-Na.Ca types. In terms of chemical composition, this water had the lowest mean concentrations of some of the main ions and K<sup>+</sup>, compared to other waters of the study area, with the exception of Ca<sup>2+</sup> and HCO<sub>3</sub><sup>-</sup>. However, its pH values were the highest. Most samples in this group were obtained in the west of the study area, near the leaning pluvial plain of Helan Mountain, and in the northeast. These phreatic water samples were found in stations where groundwater flows quickly and the depth down to groundwater is relatively large, resulting in relatively little influence of pollution discharge and evaporation, so water quality was better in this part of the study area (Figures 4 and 6).

The water samples of Cluster B were dominated by sodium, magnesium, bicarbonate and chloride, and they also had relatively high concentrations of sulfate and calcium. So the dominant hydrochemical facies are HCO<sub>3</sub>-Na.Mg, HCO<sub>3</sub>·Cl-Na.Mg and HCO<sub>3</sub>·Cl-Na types. As for chemical elements, this water type had the highest mean concentrations of HCO<sub>3</sub><sup>-</sup>, K<sup>+</sup>, NO<sub>3</sub><sup>-</sup> and F<sup>-</sup>, while Ca<sup>2+</sup> was the lowest among the clusters. Cluster B stations were found in the center of the study area (Figure 4) and had higher ion concentrations than Cluster A (except Ca<sup>2+</sup> and NH<sub>4</sub><sup>+</sup>), which may indicate that they are more influenced by evaporation than group A stations, due to run off underground. These samples were collected mainly in the vicinity of Luhuatai and Nongkesuo (in the north) and Wangyuan town, where depths down to groundwater are shallow (1 to 2.5 m), making water there more susceptible to evaporation and pollution discharge.

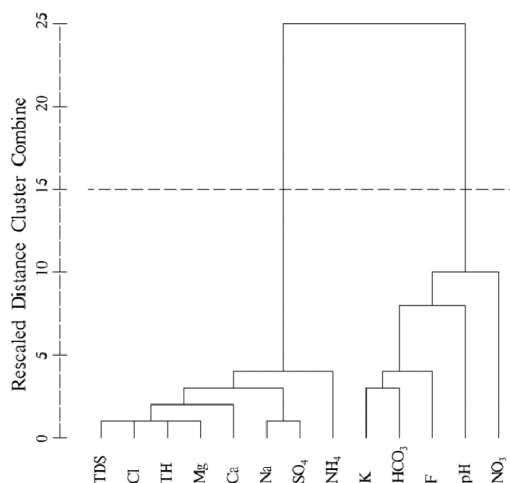
Finally, the water sample of Cluster C was dominated by sodium, magnesium and chloride, and it also had relatively high concentrations of sulfate, bicarbonate and calcium, so the hydrochemical facies is Cl-Na.Mg type. This water had the highest mean concentrations of main ions and NH<sub>4</sub><sup>+</sup>, while pH, HCO<sub>3</sub><sup>-</sup>, NO<sub>3</sub><sup>-</sup> and F<sup>-</sup> were the lowest. The single sample station of this cluster, Q45, is located east of Zhangzheng in the alluvial flat near the Yellow River. The depth to groundwater level there is less than 1.5m (Figure 4), so evaporation is high.

#### 4.4.2. R-Mode Cluster Analysis

Based on this cluster analysis of our standardized, z-transformed water quality data [17,18], there were two distinct groups or clusters of sampling stations (Figure 9). Cluster 1 represented measures of potassium ( $K^+$ ), bicarbonate ( $HCO_3^-$ ), fluoride ( $F^-$ ), nitrate ( $NO_3^-$ ) and pH. Cluster 2 represented measures of total dissolved solid (TDS), total hardness (TH), magnesium ( $Mg^{2+}$ ), calcium ( $Ca^{2+}$ ), sodium ( $Na^+$ ), chloride ( $Cl^-$ ), sulfate ( $SO_4^{2-}$ ), and ammonium ( $NH_4^+$ ).

The presence of two distinct clusters suggests that there may be two distinct sets of influences that are affecting water samples in our study area, *i.e.*, a combination of natural factors, pollution, and other human activities, known as “poles” [30]. To characterize the two poles revealed by clustering, we inferred that the influence on Cluster 1 is most likely the effect of mineral dissolution, because the concentrations of these elements increased with flow down the hydraulic gradient, from west to east. The pole for Cluster 2, however, cannot be attributed to a single factor; there may be many processes that influencing the water quality of this pole simultaneously, including natural processes such as evaporation, and anthropogenic sources such as agricultural practices. Natural processes, such as strong evaporation, as the concentrations of these main ions are not easy to precipitate with other ions during flowing underground and these ions increased greatly. The concentration of TDS for phreatic water ranged between 272 mg/L and 5664 mg/L, with only the precipitation of carbonate will occur. In addition, anthropogenic sources, such as the application of pesticides, insecticides and fertilizers in irrigation farming and domestic sewage, also exert significant impact.

**Figure 9.** Dendrogram from cluster analysis (R-mode) of 13 variables for water samples.



## 5. Conclusions

Phreatic water is an invaluable resource that supports numerous activities in the Yinchuan region, including agricultural irrigation, industry and drinking, and has done so for centuries. However, it is being heavily contaminated by human activities. This paper investigated the hydrochemistry of major ions in phreatic water samples from across the region, using methods such as correlation analysis, PCA, CA and tri-linear diagrams to assess a multivariate data set. Our comprehensive analysis of the Yinchuan region’s hydrogeological system can be summarized as follows:

1. The quality of phreatic water varied greatly across the Yinchuan region and its composition changed greatly in alluvial-lacustrine plain, the east of study area. Changes of TDS and concentrations of major ions generally increased along the hydraulic flow path, from west to east. Samples with TDS < 1 g/L were mainly from the west part of the plain, while samples in the central part of the region usually had TDS of 1 to 1.5 g/L. Moderate salt water with TDS > 1.5 g/L was located at three single areas: west of Wangyuan Town, near Luhuatai and Nongkesuo in the north, and east of Zhangzheng, along the Yellow River (Figure 5a).
2. The quality of phreatic water in study area is mainly controlled by the strong evaporation effect caused by the dry climate, dissolution of carbonate minerals and those containing F<sup>-</sup> and K<sup>-</sup>, and human activities including the treatment of industrial and municipal wastewater, the discharge of domestic sewage, and utilization of chemical fertilizer. This is confirmed by the results of correlation analysis and principal component analysis. The main hydrogeochemical processes include the strong evaporation effect caused by the dry climate, the dissolution/precipitation of limestone, dolomite and calcite. Cation exchange and dissolution of other minerals, such as fluorite, feldspar and mica, also took place. Mixing with local irrigation water can also explain some of the observed variation of ions.
3. Two types of clustering analysis helped to further characterize the water quality. CA in Q-mode identified three clusters, representing a significant gradient from A to C of increasing hydrochemical measures (except Ca<sup>2+</sup> and HCO<sub>3</sub><sup>-</sup>), from fresh water to almost saline water, which is consisted with the general flow direction (from west to east). R-mode CA revealed two distinct clusters of variables, related to two distinct sets of factors that are likely influencing Yinchuan region's phreatic water, which may include natural processes pollution, and/or other human impacts.
4. In order to improve and protect the quality of phreatic water, greater importance should be attached to water resources management and planning in the study area. In leaning pluvial plain, as TDS < 1 g/L and the concentrations of other ions are small, groundwater depth is much larger than 3 m (the extinction evaporation depth), so the evaporation effect is weak and the quality is good for drinking, agricultural irrigation and industry. In addition, the area is the recharge zone of groundwater for the whole plain, so water resources management shall be strictly performed in this area for the pollution from industrial enterprises and livestock breeding. However, in other parts, the water qualities of phreatic water have been polluted more or less due to the lessening groundwater depth and extensive influences of human activities. Therefore, the best solution is reducing the amount of evaporation by increasing pumping groundwater and decreasing canal irrigation water in irrigation period in order to reduce groundwater level into a more proper level.

## Acknowledgments

This research was supported by the Doctor Postgraduate Technical Project of Chang'an University (2013G5290003) and the National Natural Science Foundation of China (41172212). The authors would like to acknowledge the anonymous reviewers for their critical review of the manuscript and suggestions for further improvements.

## Author Contributions

The work presented here was carried out in collaboration between all authors. Zhang Xuedi and Qian Hui defined the research theme, designed methods and experiments. Chen Jie and Qiao Liang carried out the laboratory experiments. Zhang Xuedi analyzed the data, interpreted the results and wrote the paper. All authors have contributed to, seen and approved the manuscript.

## Appendix

**Table A1.** General information of samples.

Samples	pH	TH	TDS	Ca <sup>2+</sup>	Mg <sup>2+</sup>	K <sup>+</sup>	Na <sup>+</sup>	Cl <sup>-</sup>	SO <sub>4</sub> <sup>2-</sup>	HCO <sub>3</sub> <sup>-</sup>	NO <sub>3</sub> <sup>-</sup>	NH <sub>4</sub> <sup>+</sup>	F <sup>-</sup>
Q3	8.0	254.5	368	49.9	34.9	3.00	31.0	51.8	58.2	245.1	1.24	0.00	0.10
Q6	8.1	405.2	727	71.0	64.0	6.00	89.2	89.8	209.6	352.0	3.62	0.00	0.36
Q8	8.0	317.2	933	55.7	50.1	10.00	197.0	158.8	235.4	377.1	1.47	0.00	0.08
Q10	8.1	260.3	528	51.8	34.9	3.00	86.0	62.1	127.1	289.1	2.49	0.00	0.16
Q13	8.1	334.7	621	55.7	55.9	4.50	86.0	103.6	129.6	333.1	2.71	0.00	0.30
Q14	8.4	197.8	272	40.3	25.6	3.00	24.0	27.6	36.4	251.4	0.57	0.03	0.36
Q16	8.1	314.1	517	44.2	60.5	3.50	44.0	58.7	172.9	232.6	1.70	0.00	0.10
Q22	8.1	513.2	1236	115.2	55.9	3.00	268.0	281.8	272.1	465.1	0.34	0.93	0.10
Q25	8.0	789.3	1905	71.0	192.1	4.50	356.8	466.0	337.0	892.5	11.30	0.00	0.36
Q26	7.9	635.7	2200	32.6	179.3	6.00	480.0	490.2	701.9	534.2	21.47	0.00	0.10
Q27	8.1	661.1	1850	74.9	145.5	8.00	370.0	314.1	592.4	647.4	1.81	0.00	0.44
Q28	8.0	305.5	439	57.6	44.2	3.00	40.0	58.7	53.1	333.1	0.00	0.00	0.10
Q29	8.1	349.2	631	61.4	54.7	4.00	83.0	79.4	164.7	333.1	1.70	0.00	0.11
Q36	8.2	515.2	985	51.8	119.9	17.00	149.0	145.0	62.6	842.2	0.00	0.00	1.20
Q37	8.0	213.0	359	38.4	32.6	2.00	44.0	62.1	53.0	220.0	1.47	0.00	0.76
Q44	8.1	600.2	951	126.7	73.3	7.50	107.0	141.5	205.2	534.2	3.39	0.00	0.16
Q45	7.7	2845.0	5664	439.7	508.7	8.00	860.0	2592.5	986.3	440.0	0.00	1.01	0.10
Q47	8.1	201.5	290	34.4	32.6	2.50	24.0	34.5	35.2	226.3	0.36	0.00	0.08
Q48	8.0	436.4	896	76.8	68.7	3.00	138.0	148.4	256.6	358.3	8.50	0.00	0.10
Q54	8.1	571.5	969	111.4	79.2	4.00	128.0	155.3	187.6	565.7	1.47	0.00	0.30
Q57	8.1	380.9	673	65.3	61.7	3.50	86.0	34.5	159.1	471.4	0.23	0.00	0.36
Q58	8.1	474.6	810	121.0	37.3	3.00	130.4	96.7	100.5	603.4	0.90	0.00	0.10
Q61	8.1	634.4	1157	149.8	61.7	4.00	185.0	189.9	231.6	628.5	0.00	0.08	0.10
Q63	8.0	547.5	1025	99.8	82.6	5.00	138.0	231.3	295.8	308.0	1.36	0.00	0.08
Q65	8.1	332.8	600	42.2	68.7	3.00	72.0	65.6	130.3	383.4	13.56	0.00	0.10
Q68	8.2	753.2	1886	73.0	178.1	17.00	388.0	310.7	290.1	1106.2	0.00	0.00	0.64
Q72	8.1	438.0	915	101.8	44.2	3.00	174.0	145.0	146.4	553.1	0.00	0.00	0.16
Q75	8.1	511.3	988	101.8	68.7	2.00	164.0	138.1	199.5	590.8	0.11	0.00	0.16
Q77	8.1	462.3	934	69.1	85.0	5.00	153.0	110.5	156.3	653.6	0.00	0.00	0.44
Q78	8.2	555.1	1002	115.2	69.8	4.00	153.0	151.9	181.3	609.7	0.68	0.00	0.16
Q79	8.0	706.0	1217	92.2	143.2	4.50	138.0	200.2	294.9	641.1	0.57	0.00	0.40
Q81	8.1	558.6	988	115.2	71.0	4.00	153.0	145.0	188.2	565.7	0.00	0.00	0.24
Q82	8.4	467.9	1003	76.8	79.2	5.00	172.0	169.2	233.6	490.2	0.14	0.00	0.30
Q83	8.1	577.5	894	107.5	85.0	3.00	98.4	131.2	132.4	615.9	0.00	0.00	0.30
Q86	8.0	145.9	1048	23.0	25.6	1.50	344.0	359.0	95.9	364.5	0.23	0.00	0.36
Q88	8.0	242.6	397	57.6	23.3	3.00	57.0	55.2	65.2	238.8	0.00	0.00	0.08
Q91	8.2	547.3	976	105.6	76.8	2.00	144.0	127.7	168.6	647.4	0.00	0.00	0.11
Q93	8.0	307.4	1765	32.6	69.8	5.00	540.0	379.7	282.6	867.3	0.00	0.00	0.56
Q95	8.1	477.7	908	61.4	97.8	7.00	145.0	82.9	122.3	735.4	0.00	0.00	0.10

## Conflicts of Interest

The authors declare no conflict of interest.

## References

1. Brunke, M.; Gonsler, T. The ecological significance of exchange processes between rivers and groundwater. *Freshw. Biol.* **1997**, *37*, 1–33.
2. Dillon, P. J.; Kirchner, W.B. The effects of geology and land use on the export of phosphorous from watersheds. *Water Res.* **1975**, *9*, 125–148.
3. Sophocleous, M. Interactions between groundwater and surface water: The state of the science. *Hydrogeology* **2002**, *10*, 52–67.
4. Vega, M.; Pardo, R.; Barrado, E.; Deban, L. Assessment of seasonal and polluting effects on the quality of river water by exploratory data analysis. *Water Res.* **1998**, *32*, 3581–3592.
5. Qian, H.; Li, P.Y. Hydrochemical characteristics of groundwater in Yinchuan plain and their control factors. *Asian J. Chem.* **2011**, *23*, 2927–2938.
6. Jin, X.; Wan, L.; Zhang, Y.; Xue, Z.; Yin, Y. A study of the relationship between vegetation growth and groundwater in the Yinchuan Plain. *Earth Sci. Front.* **2007**, *14*, 197–203.
7. Andradea, E.M.; Palacio, H.A.Q.; Souza, I.H.; Leaoa, R.A.O.; Guerreiroc, M.J. Land use effects in groundwater composition of an alluvial aquifer (Trussu River, Brazil) by multivariate techniques. *Environ. Res.* **2008**, *106*, 170–177.
8. Reisenhofer, E.; Adami, G.; Barbieri, P. Using chemical and physical parameters to define the quality of karstic freshwaters (Timavo River, Northeastern Italy): A chemometric approach. *Wat. Res.* **1998**, *32*, 1193–1203.
9. Qian, H.; Wu, J.; Zhou, Y.H.; Li, P.Y. Stable oxygen and hydrogen isotopes as indicators of lake water recharge and evaporation in the lakes of the Yinchuan Plain. *Hydrol. Process.* **2013**, doi:10.1002/hyp.9915.
10. Liu, P.G.; Fan, S.X.; Li, X.J. The geochemical element characteristics and paleo-sedimentary environment of the Quaternary deposits in Yinchuan Basin. *J. Geomech.* **2000**, *6*, 43–50.
11. Zhang, L.; Wang, L. *Groundwater Resources in Ningxia*; Ningxia People Publishing House: Yinchuan, China, 2003.
12. Wu, X.H.; Qian, H.; Yu, D.M. *Investigation and Assessment of Rational Allocation of Groundwater Resources in the Yinchuan Plain*; Geology Publishing House: Beijing, China, 2008.
13. Lu, D.M. *History of Diverting Yellow River Water for Irrigation in Ningxia*; China Water Power Press: Beijing, China, 1987.
14. Ministry of Health of the People's Republic of China. *Standards for drinking water quality*; GB 5749-2006; Standards Press of China: Beijing, China, 2007.
15. Kaufman, L. *Finding Groups in Data: An Introduction to Cluster Analysis*; Wiley: New York, NY, USA, 1990.
16. Tang, Q.Y. *DPS© Data Processing System: Experimental Design, Statistical Analysis and Data Mining*, 2nd ed.; Science Press: Beijing, China, 2010. (In Chinese)

17. Helena, B.; Pardo, R.; Vega, M.; Barrado, E.; Fernandez, J.M.; Fernandez, L. Temporal evolution of groundwater composition in an alluvial aquifer (Pisuerga River, Spain) by principal component analysis. *Water Res.* **2000**, *34*, 807–816.
18. Willet, P. *Similarity and Clustering in Chemical Information Systems*; Research Studies Press, Wiley: New York, NY, USA, 1987.
19. Li, P.Y.; Qian, H.; Wu, J.H.; Zhang, Y.Q.; Zhang, H.B. Major ion chemistry of shallow groundwater in the Dongsheng Coalfield, Ordos Basin, China. *Mine Water Environ.* **2013**, *32*, 195–206.
20. Brown, C. *Applied Multivariate Statistics in Geohydrology and Related Science*, 1st ed.; Springer: Berlin, Germany, 1998; pp. 1–248.
21. Hopke, P.K.; Gladney, E.S.; Gordon, G.E.; Zoller, W.H.; Jones, A.G. The use of multivariate analysis to identify sources of selected elements in the Boston urban aerosol. *Atmos. Environ.* **1976**, *10*, 1015–1025.
22. Voudouris, K.; Panagopolous, A.; Koumanatakis, J. Multivariate statistical analysis in the assessment of hydrochemistry of the Northern Korinthia Prefecture alluvial system (Peloponnese, Greece). *Nat. Resour. Res.* **2000**, *9*, 135–146.
23. Hussein, M.T. Hydrochemical evaluation of groundwater in the Blue Nile Basin, eastern Sudan, using conventional and multivariate techniques. *Hydrogeol. J.* **2004**, *12*, 12–144.
24. Mahlknecht, J.; Steinich, B.; Navarro de Leon, I. Groundwater chemistry and mass transfers in the Independence aquifer, central Mexico, by using multivariate statistics and mass-balance models. *Environ. Geol.* **2004**, *45*, 781–795.
25. Hussain, M.; Ahmed, S.M.; Abderrahman, W. Cluster analysis and quality assessment of logged water at an irrigation project, eastern Saudi Arabia. *J. Environ. Manag.* **2008**, *86*, 297–307.
26. Qian, H.; Zhang, X.D.; Li, P.Y. Calculation of CaCO<sub>3</sub> solubility (precipitability) in natural waters. *Asian J. Chem.* **2012**, *24*, 668–672.
27. Li, P.Y.; Qian, H.; Wu, J.H. Hydrochemical characteristics and evolution laws of drinking groundwater in Pengyang County, Ningxia, Northwest China. *E J. Chem.* **2011**, *8*, 565–575.
28. Lucas, L.; Jauzein, M. Use of principal component analysis to profile temporal and spatial variations of chlorinated solvent concentration in groundwater. *Environ. Pollut.* **2008**, *151*, 205–212.
29. Wu, J.H.; Li, P.Y.; Qian, H.; Duan, Z.; Zhang, X.D. Using correlation and multivariate statistical analysis to identify hydrogeochemical processes affecting the major ion chemistry of waters: a case study in Laoheba phosphorite mine in Sichuan, China. *Arab. J. Geosci.* **2013**, doi:10.1007/s12517-013-1057-4.
30. Rapin, F. Anthropogenic Effects on Sediment from Bay of Nice and Villefranche-sur-Mer on the French Coast. Ph.D. Dissertation, University of Geneva, Geneva, Switzerland, 1980; p. 221.